

Scalable Quantum Walk-Based Heuristics for the Minimum Vertex Cover Problem

F. S. Luiz ,¹ A. K. F. Iwakami,¹ D. H. Moraes,² and M. C. de Oliveira ,^{1,3}

¹*Instituto de Física Gleb Wataghin, Universidade Estadual de Campinas, 13083-859, Campinas, SP, Brazil* 

²*Venturus Innovation Center, Campinas, SP, Brazil* 

³*QuaTI - Quantum Technology & Information, 13560-161, São Carlos, SP, Brazil* 

We propose a novel heuristic quantum algorithm for the Minimum Vertex Cover (MVC) problem based on continuous-time quantum walks (CTQWs). In this framework, the coherent propagation of a quantum walker over a graph encodes its structural properties into state amplitudes, enabling the identification of highly influential vertices through their transition probabilities. To enhance stability and solution quality, we introduce a dynamic decoupling (“freezing”) mechanism that isolates vertices already selected for the cover, preventing their interference in subsequent iterations of the algorithm. The method employs a compact binary encoding, requiring only $\lceil \log_2(V) \rceil$ qubits to represent a graph with V vertices, resulting in an exponential reduction of quantum resources compared to conventional vertex-based encodings. We benchmark the proposed heuristic against exact solutions obtained via Mixed-Integer Linear Programming (MILP) and against established classical heuristics, including Simulated Annealing, FastVC, and the 2-Approximation algorithm, across Erdős–Rényi, Barabási–Albert and regular random graph ensembles. Our results demonstrate that the CTQW-based heuristic consistently achieves superior approximation ratios and exhibits remarkable robustness with respect to network topology, outperforming classical approaches in both heterogeneous and homogeneous structures. These findings indicate that continuous-time quantum walks, when combined with topology-independent decoupling strategies, provide a powerful paradigm for large-scale combinatorial optimization and complex network control, with potential applications spanning infrastructure resilience, epidemic containment, sensor network optimization, and biological systems analysis.

INTRODUCTION

The *Minimum Vertex Cover* (MVC) problem is a central challenge in graph theory and combinatorial optimization, with broad relevance in disciplines such as communication networks, bioinformatics, infrastructure planning, epidemiological modeling, and circuit design [1, 2]. Given a graph $G = (V, E)$, the task is to determine a minimum-size subset of vertices $C \subseteq V$ such that every edge $e \in E$ is incident to at least one vertex in C . Despite its simple formulation, the MVC problem is NP-complete, as originally established by Karp [1], which implies that, unless $P = NP$, no polynomial-time algorithm exists for its exact solution in the general case.

Exact approaches to the MVC problem typically rely on fixed-parameter algorithms, which can achieve runtimes of the form $2^{O(k)} \cdot n^{O(1)}$ when the size of the vertex cover k is small [2, 3]. Additional strategies include branch-and-bound and exhaustive search techniques, but their applicability is considerably limited for graphs of moderate to large size due to the exponential scaling of the problem. As a result, heuristic and approximation algorithms have become essential tools in practical applications.

Among the classical approximation strategies, one of the most widely used approaches is based on constructing a maximal matching and selecting both endpoints of each matched edge, yielding a guaranteed approximation ratio of at most 2 relative to the optimal solution [4, 5]. Subsequent studies have established strong inapproximability bounds. For instance, Dinur and Safra proved that, under standard complexity-theoretic assumptions, there exists no polynomial-time algorithm capable of achieving an approximation ratio below approximately 1.3606 for graphs of sufficiently large degree [6]. These fundamental limitations highlight the intrinsic dif-

ficulty of the MVC problem and the need for new algorithmic paradigms.

In recent years, the rapid development of quantum computing has motivated the exploration of quantum and quantum-inspired algorithms for combinatorial optimization. Notably, the Quantum Approximate Optimization Algorithm (QAOA) and its extensions have been applied to the vertex cover problem and related formulations [7–9]. Variants such as the Quantum Alternating Operator Ansatz and quantum generalizations of the problem, including the Transverse Vertex Cover model, recast the task as the minimization of a Hamiltonian with non-classical interactions [10, 11]. Although these approaches offer new avenues for exploration, they still face fundamental limitations as well as practical barriers related to hardware noise, circuit depth, and the large number of qubits required for useful implementations.

Indeed, most current quantum devices operate in the so-called Noisy Intermediate-Scale Quantum (NISQ) regime, characterized by a limited number of qubits and non-negligible decoherence [12–14]. Reliable fault-tolerant quantum computation may require millions of physical qubits, which remains beyond present technological capabilities. Consequently, the immediate impact of quantum computing is likely to arise not only from hardware advances, but also from the development of resource-efficient algorithms that can operate within NISQ constraints or that can be simulated efficiently on classical machines while preserving a clear roadmap towards quantum implementation [15–17].

Within this context, quantum walks have emerged as a powerful theoretical and algorithmic framework. Continuous-Time Quantum Walks (CTQWs), in particular, are governed by a Hamiltonian directly related to the Laplacian of a graph and exhibit rich dynamical behavior shaped by interference,

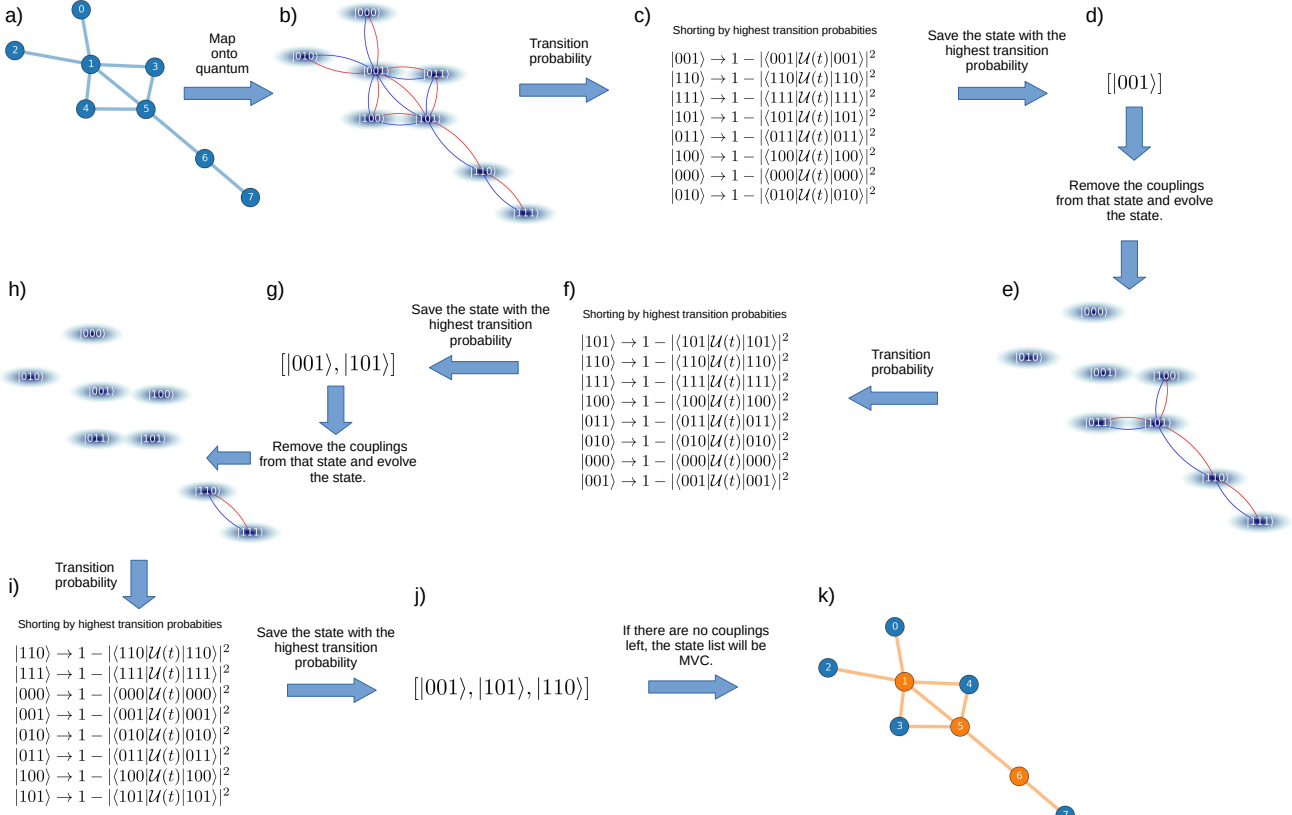


Figure 1. Iterative Quantum Walk Protocol for MVC. The figure illustrates the sequential algorithm for determining the MVC. (a) An initial graph is defined. (b) The graph is mapped onto quantum states using binary encoding, and the system is evolved via a Quantum Walk. (c-d) Transition probabilities between states are calculated, and the state with the highest probability is identified and saved. (e-g) Iterative Decoupling: The saved state is decoupled from the remaining system, which is then evolved again. The next state with the highest transition probability is selected and saved. (h-j) This decoupling and selection process continues iteratively, identifying the next most probable state. (k) Final Solution: The iteration stops when all remaining states are decoupled (i.e., no more couplings exist between them). The collection of all saved states represents the MVC for the initial graph.

superposition, and coherence [18–20]. These properties have been exploited in a range of quantum algorithms, including spatial search, element distinctness, and graph-based problems [21]. Recently, we demonstrated that CTQWs can be leveraged to solve the Minimum Spanning Tree problem under degree constraints, where vertices with larger transition probabilities naturally emerged as structurally relevant [22].

In the context of the Minimum Vertex Cover problem, an optimal solution is expected to contain vertices whose removal most effectively reduces the graph's edge connectivity. Within a CTQW framework, such vertices manifest as quantum states exhibiting large transition probabilities, since they correspond to locations from which the quantum amplitude can efficiently spread through the network. This observation establishes a direct physical connection between quantum transport dynamics and classical notions of vertex centrality and structural importance, providing a principled foundation

for a CTQW-based heuristic for MVC.

In this work, we introduce a novel heuristics for the Minimum Vertex Cover problem based on Continuous-Time Quantum Walks. The algorithm operates iteratively: at each step, the graph is encoded into a Hamiltonian via its normalized Laplacian, the quantum system evolves over a short optimal time, and the vertex corresponding to the highest transition probability is selected as part of the cover. To prevent interference from previously selected vertices, we introduce a dynamic decoupling (or “freezing”) mechanism that effectively removes these vertices from the subsequent evolution. This combination of quantum propagation and selective decoupling enables the systematic construction of a vertex cover while preserving the essential structure of the remaining graph.

A key feature of our approach is its high resource efficiency. By employing a binary encoding of vertex indices, the algorithm requires only $\lceil \log_2(V) \rceil$ qubits to represent a graph with

V vertices, in contrast to conventional methods that typically require one qubit per vertex. This exponential reduction in qubit requirements allows the algorithm to be simulated efficiently on classical hardware for medium-sized graphs and indicates its strong potential for future implementation on scalable quantum platforms.

To evaluate the robustness and generality of the proposed method, we benchmark its performance against exact solutions obtained via Mixed-Integer Linear Programming (MILP) and against established classical heuristics, including Simulated Annealing, FastVC, and the 2-Approximation algorithm. The tests are conducted on three fundamental classes of graphs — Erdős–Rényi, Barabási–Albert, and Regular networks — covering a wide range of structural properties, from homogeneous to scale-free and highly symmetric topologies.

Our analysis reveals that the CTQW-based heuristic consistently achieves superior approximation ratios and maintains remarkable robustness with respect to network topology. These results suggest that continuous-time quantum walk dynamics, combined with topology-independent decoupling strategies, constitute a powerful and general paradigm for large-scale combinatorial optimization and complex network analysis.

The remainder of this paper is organized as follows. In Sec. II we introduce the graph-to-Hamiltonian mapping and the quantum walk formalism. In Sec. III we describe the dynamic decoupling mechanism and the full iterative heuristic. Sec. IV presents the numerical results and a comparative performance analysis. In Sec. V and Sec. VI we discuss broader implications for complex systems and real-world applications. Finally, we conclude in Sec. VII with a summary and outlook on future directions.

METHODS

The MVC problem is an NP-hard combinatorial optimization problem defined on a graph $G = (V, E)$, where V is the set of vertices and E is the set of edges. A vertex cover $C \subseteq V$ is a subset of vertices such that for every edge $(u, v) \in E$, at least one of its endpoints, u or v , is in C . This condition can be formally expressed as $\forall (u, v) \in E \{u, v\} \cap C \neq \emptyset$. The objective is to find a vertex cover C with minimal cardinality, referred to as the MVC. Given the inherent computational complexity of finding an exact solution, our study introduces a novel, resource-efficient heuristic that leverages the dynamics of continuous-time quantum walks.

To minimize quantum resources, we encode the graph vertices using a binary representation. This allows us to represent the V vertices using only $\lceil \log_2(V) \rceil$ qubits. The edges of the graph are mapped to the possible transitions between these encoded quantum states. Figure 1a and 1b illustrates the encoding for an 8-vertex graph, which requires 3 qubits. The vertices are represented by their corresponding binary states: $0 \leftrightarrow |000\rangle$, $1 \leftrightarrow |001\rangle$, $2 \leftrightarrow |010\rangle$, $3 \leftrightarrow |011\rangle$, $4 \leftrightarrow |100\rangle$, $5 \leftrightarrow |101\rangle$, $6 \leftrightarrow |110\rangle$ and $7 \leftrightarrow |111\rangle$.

A. Hamiltonian and Graph Encoding

The evolution of this system encoded in a quantum system is described by the system's Hamiltonian. In continuous-time quantum walk, the Hamiltonian is mapped to the graph's Laplacian [18–20]. The Laplacian of a graph contains all the information about the graph; it is composed of the degree matrix and the adjacency matrix, as in $L = D - A$. Where the elements of the adjacency matrix A are

$$A_{ij} = \begin{cases} 1, & \{i, j\} \in E \\ 0, & \text{otherwise.} \end{cases} \quad (1)$$

and the elements of the degree matrix are given by

$$D_{ij} = \delta_{ij} \sum_k A_{ik}. \quad (2)$$

In our approach, we use the normalized symmetric Laplacian, $L_{sym} = D^{-1/2} L D^{-1/2} = \mathbf{I} - D^{-1/2} A D^{-1/2}$. This choice is motivated by its ability to model a more uniform propagation dynamic across the graph [23, 24]. By using the normalized Laplacian, our heuristic is less biased towards high-degree vertices. The probability of transitioning to a neighbor is treated more fairly, providing a clearer view of each vertex's importance in the propagation of the quantum state.

With the Laplacian defined, we map the Hamiltonian of our quantum system directly onto L_{sym} , so the Hamiltonian can be written as:

$$\mathcal{H} = \sum_i |i\rangle\langle i| - \sum_{i,j} \frac{A_{ij}}{\sqrt{D_{ii}D_{jj}}} |i\rangle\langle j| \quad (3)$$

This Hamiltonian can also be written in a more general form, $H \equiv \gamma I - \epsilon \Gamma$, where the constants ϵ and γ modulate the transition strength (related to adjacency) and the local energy (related to the identity operator) and $\Gamma_{ij} = \frac{A_{ij}}{\sqrt{D_{ii}D_{jj}}}$. For our purposes, we operate in natural units, which allows us to set $\epsilon = \gamma = 1$.

B. Quantum Walk Dynamics and Transition Probabilities

The evolution of the CTQW system is governed by the time-independent Schrödinger equation, where the evolution operator is given by $U(t) = e^{-i\mathcal{H}t}$ (assuming $\hbar = 1$). This evolution enables the quantum state to explore multiple paths simultaneously, a key advantage over classical random walks [21]. However, this also introduces the well-known challenge of quantum interference. As the quantum walker superposition evolves, the amplitudes can return to the same site, leading to constructive and destructive interference. Over longer periods, this interference can cause the quantum state to become localized or to obscure valuable information about the graph's overall structure.

To mitigate this problem, our method employs an optimal evolution time, t_{opt} . This time is carefully chosen to be short enough to allow the superposition to propagate across the entire graph, but not so long that destructive interference dominates the dynamics. Based on our previous work [22], we set this time as:

$$t_{opt} = \frac{4}{\pi\sqrt{V}} + 0.1. \quad (4)$$

At the end of this evolution, our heuristic evaluates the probability of the state transitioning away from its initial vertex. This transition probability for an initial state $|m\rangle$ is given by $P(m \rightarrow \text{out}) = \sum_{j \neq m} P(j|m) = 1 - |\langle m|\mathcal{U}(t_{opt})|m\rangle|^2$, which measures the likelihood of the quantum walker moving to any other vertex after time t_{opt} . This metric helps us identify the most "connected" or influential vertices within the graph. To perform this calculation analytically, we take advantage of the short evolution time and approximate the evolution operator using a Trotter-Suzuki decomposition. This yields a probability of transition away from the initial state given by:

$$P(m \rightarrow \text{out}) = 1 - |(e^{it_{opt}\Gamma})_{mm}|^2, \quad (5)$$

where Γ is the matrix with elements $\Gamma_{ij} = \frac{A_{ij}}{\sqrt{D_{ii}D_{jj}}}$ and the subindex mm denotes the element in the m -th row and m -th column of the resulting exponential matrix. This approximation allows us to relate the transition probability directly to the graph's properties, providing a computationally efficient way to identify the best candidates for our MVC solution.

C. Modeling Vertex Removal with Dynamic Decoupling

Our heuristic is an iterative process that requires removing a selected vertex and its incident edges from the graph after each step. In the context of a quantum system, this process corresponds to the dynamic decoupling of the chosen vertex from the rest of the graph. This is achieved by updating the system's Hamiltonian to reflect the changes in the graph's connectivity. Specifically, for a chosen vertex m , all elements in the adjacency matrix A corresponding to its connections are set to zero ($A_{j,m} = A_{m,j} = 0$ for all neighbors j). By modifying the adjacency matrix, we create a new, modified Hamiltonian for the next iteration, which guides the quantum walk to explore the remaining parts of the graph. This approach is efficient in a classical simulation of the system.

For implementation on a quantum computer, we must utilize a more physically realistic mechanism for vertex removal, such as a freezing mechanism [25]. This mechanism effectively isolates the chosen vertex's state by adding a local term to the Hamiltonian, creating a large energy gap that prevents it from participating in the quantum dynamics. This can be achieved by rewriting the total Hamiltonian as a sum of three

components:

$$\mathcal{H}_{total} = \mathcal{H}_j + \mathcal{H}_m + \mathcal{H}_F \quad (6)$$

where \mathcal{H}_j is the Hamiltonian component that acts on the subspace of states not yet chosen for the cover, \mathcal{H}_m acts on the subspace of states already chosen, and \mathcal{H}_F is the freezing Hamiltonian. These components are defined using projection operators, $P_j = \sum_{k \notin C} |k\rangle\langle k|$ and $P_m = \sum_{k \in C} |k\rangle\langle k|$, where C is the set of chosen vertices.

The Hamiltonian for the dynamic portion of the graph is given by $\mathcal{H}_j = P_j \mathcal{H} P_j$. The Hamiltonian for the chosen, now inactive, states is $\mathcal{H}_m = P_m \mathcal{H} P_m$. Finally, the freezing Hamiltonian is an external term designed to prevent transitions into the subspace of frozen states:

$$\mathcal{H}_F = (\Omega - 1) \cdot P_m \quad (7)$$

where Ω is a large constant (penalty term). In the interaction picture, where the dynamics of \mathcal{H}_j are factored out, the evolution of the states in the frozen subspace, $|\psi_{I,m}(t)\rangle$, is governed by a Hamiltonian that contains the large energy penalty from \mathcal{H}_F . For sufficiently large Ω , the evolution of the frozen states is effectively halted. The system's evolution is then governed entirely by the remaining dynamic states:

$$i \frac{\partial |\psi_{I,j}(t)\rangle}{\partial t} \approx \mathcal{H}_j |\psi_{I,j}(t)\rangle$$

This process ensures that the quantum walk explores only the remaining part of the graph in subsequent iterations.

D. Iterative Heuristics

Our algorithm is an iterative heuristic that constructs the vertex cover step-by-step. The process can be visualized using the example in Figure 1 and is described by the following steps:

- 1. Problem Mapping:** The vertex cover problem is mapped onto a graph $G = (V, E)$ (Figure 1a). The quantum system's dynamics are then defined by a Hamiltonian, \mathcal{H} , which is constructed from the graph's Laplacian (Figure 1b).
- 2. System Evolution and Evaluation:** The quantum system evolves under the Hamiltonian's action. In each iteration, the **transition probabilities** for all vertices are calculated after an optimal evolution time, t_{opt} (Figure 1c, 1f e 1i).
- 3. Vertex Selection:** The vertex with the highest transition probability is identified and added to the current cover set (Figure 1d, 1e e 1j).
- 4. Dynamic Decoupling:** The selected vertex and its incident edges are **dynamically decoupled** from the system (Figure 1e, e 1h).

5. **Repetition:** Steps 2 through 4 are repeated on the modified graph (Figure 1e and 1h) until all edges have been covered. The process terminates when no edges remain in the graph (Figure 1h).

In order to operationalize our heuristic approach, we propose two algorithmic formulations: a conceptual quantum algorithm, which describes the evolution of the graph as a quantum system, and its classical counterpart, where transition probabilities are directly computed from the Hamiltonian. Both formulations share the same iterative strategy: vertices with the highest probability contributions are incrementally added to the cover until all edges are covered.

E. Quantum heuristic formulation

The first algorithm (Algorithm 1) highlights the quantum nature of the heuristic. The graph is encoded into a Hamiltonian $H = D - A$, the quantum state evolves under continuous-time quantum walk dynamics, and transition probabilities guide the selection of vertices. This formulation emphasizes how the graph is treated as a quantum system.

Algorithm 1: Quantum heuristic for MVC (conceptual)

Input: Graph $G(V, E)$, initial state $|\psi(0)\rangle$, evolution time t

Output: Vertex cover C

Initialize quantum state $|\psi(0)\rangle$ uniformly over V ;
Construct Hamiltonian $H = D - A$ from G ;

while there are uncovered edges in E **do**

 Evolve state: $|\psi(t)\rangle = e^{-iHt}|\psi(0)\rangle$;

 Compute transition probabilities

$$p_{ij}(t) = |\langle j|\psi(t)\rangle|^2;$$

 Select vertex v with highest probability contribution to uncovered edges;

 Add v to cover set C ;

 Remove all edges incident to v from E ;

return C ;

F. Classical simulation of the quantum walk

Although Algorithm 1 is conceptually quantum, its simulation can be efficiently performed on classical hardware for small to medium-sized instances. In this case, the state evolution is not physically realized; instead, transition probabilities are directly computed from the closed-form expression (Eq. (5)). This avoids the need for explicitly constructing the Hamiltonian as input, since H is already encoded in the Laplacian. The resulting iterative procedure is summarized in Algorithm 2.

Algorithm 2: Classical simulation of the quantum walk heuristic

Input: Graph Laplacian L , evolution time t

Output: Vertex cover C

Initialize cover set $C = \emptyset$;

while there are uncovered edges in E **do**

 For each pair (i, j) compute probability

$$P(i \rightarrow \text{out});$$

 Aggregate vertex scores;

$$\text{Select vertex } v^* = \arg \max_v s(v);$$

 Add v^* to C ;

 Remove all edges incident to v^* from E ;

return C ;

RESULTS AND DISCUSSION

To assess the robustness and generality of our algorithm, we employed three complementary classes of synthetic random graphs: *Erdős–Rényi* (ER), *Barabási–Albert* (BA) and *Regular* (REG) [26–29]. These models differ substantially in their generative mechanisms and topological properties, thus providing distinct benchmarks for performance evaluation.

Erdős–Rényi graphs were generated with node counts ranging from $N = 4$ to $N = 154$, and edge probabilities selected from the set

$$p \in \{0.2, 0.4, 0.5, 0.6, 0.7, 0.8, 0.9\}.$$

For each configuration (N, p) , 10 independent instances were sampled using different pseudo-random seeds. In the rare cases where the ER graphs were disconnected, we substituted them with *Watts–Strogatz* graphs of comparable size and density, ensuring connectivity while preserving a similar level of randomness. ER graphs serve as a baseline of homogeneous random connectivity, where the degree distribution is binomial (or approximately Poisson in the sparse regime).

Barabási–Albert graphs were generated to evaluate the algorithm’s sensitivity to degree heterogeneity and scale-free structures. In this model, networks grow dynamically: starting from a small connected core of m_0 nodes, each newly added node attaches to m existing nodes with probability proportional to their degree (preferential attachment). This mechanism yields scale-free networks characterized by a power-law degree distribution $P(k) \sim k^{-3}$, in sharp contrast to the homogeneous distribution of ER graphs. In our simulations, we considered networks with $N = 4$ to $N = 154$, varying the connectivity parameter as

$$m \in \{1, 2, 3, 5, 10, 15\}.$$

To further analyze the dependence of algorithmic performance on network topology, we also generated *regular* graphs, in which all vertices have the same degree k . These graphs provide a homogeneous benchmark that iso-

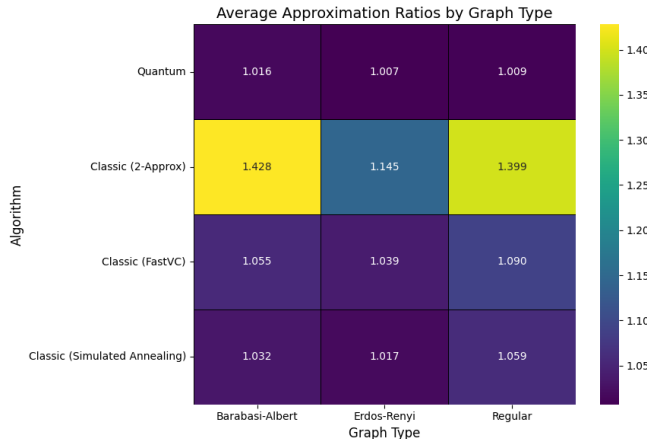


Figure 2. Heatmap showing the average approximation ratio for the Quantum, FastVC, Simulated Annealing (SA), and 2-Approximation algorithms. The ratio is defined as the size of the algorithm’s solution divided by the exact MVC size, which was computed using Mixed-Integer Linear Programming (MILP). Mean values were calculated over a set of graph instances for each topology. Ratios closer to 1.0 indicate superior average performance and higher solution quality.

lates the effects of topological heterogeneity observed in the Erdős–Rényi and Barabási–Albert models. To analyze homogeneous topologies, we generated regular graphs in which every vertex has the same degree k . For each network size $N \in [4, 154]$, we considered degrees k approximately corresponding to $2, 0.25N, 0.5N$, ensuring that $(N \times k)$ was even to make the regular graph feasible. For each (N, k) configuration, up to five distinct connected graphs were generated, verified to be non-isomorphic using the Weisfeiler–Lehman graph hash. Regular graphs are particularly relevant for CTQW-based heuristics because their uniform Laplacian spectra lead to well-defined dispersion properties, reducing localization effects and providing a baseline for assessing how structural heterogeneity (as in BA or ER graphs) influences quantum dynamics and optimization outcomes.

This dataset complements the analysis by enabling a systematic comparison across random, scale-free, and uniform connectivity regimes. For each configuration (N, m) , 10 graph instances were generated using different random seeds, resulting in a diverse set of topologies with heterogeneous degree structures.

In all models, edge weights were fixed to $w_{ij} = 1.0$ to eliminate weight heterogeneity and focus the analysis exclusively on structural and topological factors. Each graph instance was then used in two computational scenarios:

1. **Quantum simulation**, where the system evolved under a Hamiltonian given by the graph Laplacian, following a Continuous-Time Quantum Walk (CTQW) up to $t_{\max} = 0.01$;
2. **Exact classical resolution** of the Vertex Cover problem with Mixed Integer Linear Programming (MILP).

3. Classic heuristics algorithms: 2-Approx, FastVC and Simulated Annealing.

This framework allowed us to systematically compare the proposed quantum heuristic against classical methods across networks of varying density (ER) and heterogeneous degree distributions (BA). In particular, ER graphs provided insights into algorithmic performance under uniform connectivity, while BA graphs revealed how degree heterogeneity and hub formation impact solution quality and scalability. In contrast to the Erdős–Rényi and Barabási–Albert models, which exhibit varying degrees of topological randomness and heterogeneity, regular graphs provide a controlled topology where all vertices have identical degree. This allows isolating the effects of structural symmetry on the algorithmic performance.

When generating random graphs, multiple topologies share the same number of nodes but differ in their connectivity structure. Therefore, our first analysis focuses on the average approximation ratios, defined as $\text{MVC}/\text{MVC}_{\text{exact}}$, for the Quantum algorithm (based on the Trotter–Suzuki Approximation), 2-Approx, FastVC, and Simulated Annealing methods across the Barabási–Albert (BA), Erdős–Rényi (ER), and Regular (REG) graph ensembles (see Fig. 2). Ratios closer to unity indicate superior performance, i.e., solutions approaching the exact MVC obtained via Mixed-Integer Linear Programming (MILP).

Overall, the quantum algorithm consistently achieves the highest approximation ratios across all topologies. For Erdős–Rényi graphs, the Simulated Annealing method performs closest to the quantum approach, while FastVC and 2-Approx remain slightly suboptimal. In contrast, all classical algorithms degrade significantly on Regular graphs, suggesting that their search heuristics are affected by the uniformity of connectivity and the reduced structural variability inherent to these networks.

To further investigate the influence of network structure, we examined how the average $\text{MVC}/\text{MVC}_{\text{exact}}$ ratio varies with graph size (N) and topological class. Figure 3 shows the mean ratios for all algorithms, along with ± 1 standard deviation, highlighting how performance evolves as the number of nodes increases.

Erdős–Rényi graphs. For ER graphs, the quantum and Simulated Annealing algorithms achieve the best approximation ratios, remaining near-optimal as N increases. The 2-Approx and FastVC algorithms converge more slowly toward the optimal ratio, reflecting their limited ability to exploit random connectivity. In ER graphs, where degree distributions are binomial and spectral properties are moderately heterogeneous, the CTQW efficiently explores all vertices, maintaining a consistent advantage over classical heuristics.

Barabási–Albert graphs. For BA graphs, the performance differences become more pronounced. The quantum algorithm remains stable with ratios close to one even as the system size grows, indicating robustness to degree heterogeneity. Simulated Annealing performs comparably for small graphs but stabilizes at suboptimal values for larger systems. FastVC

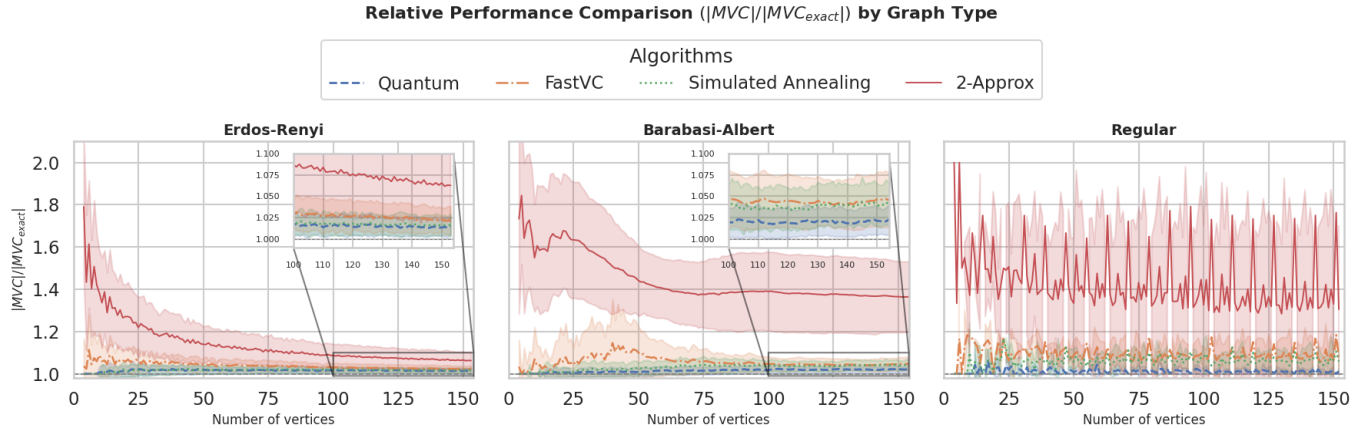


Figure 3. Average Performance and Statistical Dispersion of Approximation Ratios as a Function of Graph Size.

The figure displays the average approximation ratio achieved by the Quantum (blue), FastVC (orange), Simulated Annealing (SA) (green), and 2-Approximation (red) algorithms for the MVC problem as a function of the number of nodes (N). The analysis is segmented across three graph topologies: **Erdos-Renyi**, **Barabasi-Albert**, and **Regular**. The data was generated from 10 randomized graph instances per node count (N). The central line represents the mean ratio, while the shaded region indicates the ± 1 standard deviation (σ), reflecting the statistical dispersion of the algorithms’ performance due to the stochastic nature of the graph generation. The approximation ratio is defined relative to the exact MVC, obtained via the MILP solver. Ratios closer to 1.0 (indicated by the dashed line) denote superior average performance.

initially underperforms for small graphs, worsens around $N \approx 40$, and then partially recovers. This non-monotonic behavior likely reflects the influence of *hub nodes* in BA topologies [28]: classical heuristics often overfit to these high-degree vertices, while the quantum dynamics, driven by the CTQW Hamiltonian, distribute amplitude more evenly across the network, mitigating hub bias.

Regular graphs. In Regular graphs, where all vertices share the same degree, the quantum algorithm exhibits a clear advantage over all classical baselines. The homogeneity of connectivity induces spectral degeneracies in the Laplacian, leading to slower mixing dynamics for classical heuristics that depend on random search or local updates. The quantum evolution, however, benefits from coherent superposition: while all paths are structurally equivalent, the interference pattern stabilizes quickly, resulting in reduced oscillations of the approximation ratio as N increases. In contrast, Simulated Annealing and FastVC display persistent oscillations around a suboptimal plateau ($MVC/MVC_{exact} \approx 1.15$), indicating sensitivity to topological uniformity. Interestingly, the 2-Approx algorithm stabilizes around the same value observed in BA graphs, reinforcing its structural bias.

Topological dependence. Figure 3 highlights that the quantum algorithm exhibits remarkable topological independence, maintaining near-optimal performance regardless of the network class. This robustness stems from the underlying mechanism of the CTQW. During the short evolution period ($t_{max} = 0.01$), the quantum walker propagates coherently across the network, generating local correlations—such as short-range entanglement—without sufficient time for destructive interference to obscure structural information. By subsequently measuring the transition probabilities, the algorithm effectively identifies and decouples relevant ver-

tices. This decoupling prevents information from previous selections from contaminating subsequent decisions, ensuring stability across heterogeneous and homogeneous topologies alike.

In summary, while classical heuristics exhibit clear dependencies on structural features—randomness in ER, hub dominance in BA, and spectral uniformity in REG—the CTQW-based quantum heuristic remains largely invariant to these effects. This suggests that its performance advantage arises from the intrinsic ability of quantum evolution to sample and correlate the network structure in a balanced and topology-agnostic manner.

DATA AVAILABILITY

SOFTWARE AVAILABILITY

CONCLUSION

In this work, we presented an innovative heuristic quantum algorithm for solving the MVC problem. The algorithm is based on CQWs, where quantum propagation allows the system to probe the graph’s structure and generate correlations that encode structural information. During evolution, these correlations assist in identifying relevant vertices. The decoupling mechanism, applied after each vertex selection, prevents previously chosen vertices from introducing noise into subsequent decisions, ensuring that the quantum walk continues to explore the remaining structure efficiently.

This combination of controlled quantum propagation and vertex decoupling makes our approach robust to variations in graph topology, as confirmed by our comparative analy-

sis across Erdős–Rényi, Barabási–Albert, and Regular graphs. While classical algorithms exhibit strong dependence on topological properties such as degree heterogeneity and structural symmetry, our quantum algorithm maintains consistent performance across all regimes.

Additionally, the algorithm admits a compact binary encoding, requiring only ($\lceil \log_2(V) \rceil$) qubits to represent the vertex space. This feature allows for efficient simulations on current classical hardware and indicates potential scalability. For instance, with up to 30 noiseless qubits, it is theoretically possible to simulate graphs with up to $2^{30} \approx 1.07 \times 10^9$ vertices, illustrating the method's potential for large-scale applications.

Overall, our results demonstrate that continuous quantum walks, when combined with a topology-independent selection process, can provide a powerful heuristic framework for combinatorial optimization. Future work will focus on exploring noise effects, hybrid quantum-classical implementations, and potential extensions to other NP-hard graph problems.

FSL thanks UNICAMP Postdoctoral Researcher Program for financial support. MCO acknowledge financial support from the National Institute of Science and Technology for Applied Quantum Computing through CNPq process No. 408884/2024-0 and by FAPESP, through the Center for Research and Innovation on Smart and Quantum Materials (CRISQuM) process No. 2013/07276-1.

* fsluiz@unicamp.br

† daniel.moraes@venturus.org.br

‡ marcos@ifi.unicamp.br

[1] R. M. Karp, Reducibility among combinatorial problems, in *Complexity of Computer Computations: Proceedings of a symposium on the Complexity of Computer Computations, held March 20–22, 1972, at the IBM Thomas J. Watson Research Center, Yorktown Heights, New York, and sponsored by the Office of Naval Research, Mathematics Program, IBM World Trade Corporation, and the IBM Research Mathematical Sciences Department*, edited by R. E. Miller, J. W. Thatcher, and J. D. Bohlinger (Springer US, Boston, MA, 1972) pp. 85–103.

[2] J. Flum and M. Grohe, *Parameterized Complexity Theory* (Springer, 2006).

[3] M. Cygan, F. Fomin, Ł. Kowalik, D. Lokshtanov, D. Marx, M. Pilipczuk, M. Pilipczuk, and S. Saurabh, *Parameterized Algorithms* (Springer International Publishing, 2015).

[4] C. H. Papadimitriou and K. Steiglitz, *Combinatorial Optimization: Algorithms and Complexity* (Dover Publications, 1998).

[5] D. Hochbaum, *Approximation Algorithms for NP-hard Problems*, Computer science (PWS Publishing Company, 1997).

[6] I. Dinur and S. Safra, On the hardness of approximating minimum vertex cover, *Journal of the ACM* **52**, 1 (2005).

[7] E. Farhi, J. Goldstone, S. Gutmann, and L. Zhou, The Quantum Approximate Optimization Algorithm and the Sherrington–Kirkpatrick Model at Infinite Size, *Quantum* **6**, 759 (2022), published: 2022-07-07.

[8] K. Blekos, D. Brand, A. Ceschini, C.-H. Chou, R.-H. Li, K. Pandya, and A. Summer, A review on quantum approximate optimization algorithm and its variants, *Physics Reports* **1068**, 1 (2024), a review on Quantum Approximate Optimization Al-

gorithm and its variants.

[9] S. Hadfield, Z. Wang, B. O’Gorman, E. G. Rieffel, D. Venturelli, and R. Biswas, From the quantum approximate optimization algorithm to a quantum alternating operator ansatz, *Algorithms* **12**, 10.3390/a12020034 (2019).

[10] J. Cook, S. Eidenbenz, and A. Bärtschi, The quantum alternating operator ansatz on maximum k-vertex cover, <https://arxiv.org/abs/1910.13483> (2019), arXiv:1910.13483.

[11] S. Bravyi and M. B. Hastings, On the complexity of the quantum ising model, *Communications in Mathematical Physics* **349**, 1 (2017).

[12] J. Preskill, Quantum computing in the nisq era and beyond, *Quantum* **2**, 79 (2018).

[13] S. Chen, J. Cotler, H.-Y. Huang, and J. Li, The complexity of nisq, *Nature Communications* **14**, 6001 (2023).

[14] J. W. Z. Lau, K. H. Lim, H. Shrotriya, and L. C. Kwek, Nisq computing: where are we and where do we go?, *AAPPS Bulletin* **32**, 27 (2022).

[15] M. Ramezani, S. Salami, M. Shokhmkar, M. Moradi, and A. Bahrampour, Reducing the number of qubits from n^2 to $n \log_2(n)$ to solve the traveling salesman problem with quantum computers: A proposal for demonstrating quantum supremacy in the nisq era, arXiv preprint arXiv:2402.18530 10.48550/arXiv.2402.18530 (2024).

[16] K. Miyamoto and K. Shiohara, Reduction of qubits in a quantum algorithm for monte carlo simulation by a pseudo-random-number generator, *Phys. Rev. A* **102**, 022424 (2020).

[17] C. Chevignard, P.-A. Fouque, and A. Schrottenloher, Reducing the number of qubits in quantum factoring, *Cryptology ePrint Archive*, Paper 2024/222 (2024).

[18] E. Farhi and S. Gutmann, Quantum computation and decision trees, *Phys. Rev. A* **58**, 915 (1998).

[19] A. M. Childs, On the relationship between continuous- and discrete-time quantum walk, *Communications in Mathematical Physics* **294**, 581 (2009).

[20] S. E. Venegas-Andraca, Quantum walks: a comprehensive review, *Quantum Information Processing* **11**, 1015 (2012).

[21] J. Kempe, Quantum random walks: An introductory overview, *Contemporary Physics* **44**, 307 (2003).

[22] F. S. Luiz, F. F. Fanchini, Victor Hugo C. de Albuquerque, J. P. Papa, and M. C. de Oliveira, A quantum walk-driven algorithm for the minimum spanning tree problem under a maximal degree constraint (2025), arXiv:2508.07007 [quant-ph].

[23] A. E. Brouwer and W. H. Haemers, *Spectra of Graphs*, 1st ed., Universitext (Springer New York, NY, New York, NY, 2012) pp. XIV, 250.

[24] F. Chung, *Spectral Graph Theory*, CBMS Regional Conference Series No. N° 92 (Conference Board of the Mathematical Sciences, 2017).

[25] L. K. Castelano, I. Cunha, F. S. Luiz, R. de Jesus Napolitano, M. V. d. S. Prado, and F. F. Fanchini, Combining physics-informed neural networks with the freezing mechanism for general hamiltonian learning, *Phys. Rev. A* **110**, 032607 (2024).

[26] B. Bollobas and P. Erdős, Cliques in random graphs, *Mathematical Proceedings of the Cambridge Philosophical Society* **80**, 419–427 (1976).

[27] M. Karoński and A. Ruciński, The origins of the theory of random graphs, in *The Mathematics of Paul Erdős I*, edited by R. L. Graham and J. Nešetřil (Springer Berlin Heidelberg, Berlin, Heidelberg, 1997) pp. 311–336.

[28] A.-L. Barabási and R. Albert, Emergence of scaling in random networks, *Science* **286**, 509 (1999).

[29] W. Chen, *Graph Theory and Its Engineering Applications*, Ad-

vanced series in electrical and computer engineering (World Scientific, 1997).